PHYSICAL REVIEW B **67**, 220101(R) (2003)

Anisotropy of Co nanoparticles induced by swift heavy ions

C. D'Orléans,[1,2] J. P. Stoquert,[1] C. Estournès,[2] C. Cerruti,[3] J. J. Grob,[1] J. L. Guille,[2] F. Haas,[3] D. Muller,[1] and M. Richard-Plouet[2]

[1]*Laboratoire PHASE (UPR 292 du CNRS), 23 rue de Loess, BP 20 CR, 67037 Strasbourg Cedex 2, France*

[2]*IPCMS-GMI (UMR 75040 CNRS et ULP), 23 rue du Loess, 67037 Strasbourg Cedex 2, France*

[3]*IReS (UMR 7500 CNRS-IN2P3 et ULP), 23 rue du Loess, 67037 Strasbourg Cedex 2, France*

(Received 10 April 2003; published 18 June 2003; corrected 30 June 2003)

Spherical metallic nanoparticles have been formed in SiO_2 layers by 160-keV implantation of Co ions at a fluence of 10^{17} ions cm^{-2}. The implanted samples were next irradiated with 200-MeV ^{127}I at fluences ranging from 10^{11} to 10^{14} ions cm^{-2} at room temperature. Modifications of nanoparticle size and shape were observed by transmission-electron microscopy and have been characterized by magnetic measurements at 295 and 5 K. For ^{127}I fluences below 10^{12} ions cm^{-2}, the nanoparticles grow in size but remain spherical. For higher fluences an anisotropic growth occurs, with elongation and the preferential easy axis seen along the incident-beam direction. The nanoparticle's growth and deformations are attributed to thermal spike effects.

DOI: 10.1103/PhysRevB.67.220101 PACS number(s): 61.82.Rx, 61.46.+w, 81.07.−b, 81.16.−c

I. INTRODUCTION

Clusters can be considered as intermediate states of matter with microscopic aspects, presenting analogies with nuclei, atoms, molecules, and macroscopic properties described by thermodynamic equilibrium in condensed matter.[1] It is of fundamental interest to understand how mesoscopic organization and properties behave under high electronic excitation as a function of cluster size and shape in bulk material.

It has previously been shown that fragmentation of free clusters, surface-deposited islands, and metal colloids under high power laser irradiation occurs.[2] In such conditions, cluster explosion is attributed to photofragmentation and Coulomb fission resulting from plasmon and electron excitations induced by the incident photon beam. Related to the microscopic high power deposition, ionization, charge transfer, and evaporation of metallic clusters have been observed.

Energetic heavy ions offer an alternative to photons for introducing electronic excitations into materials. By interacting strongly with the electrons located within a few nanometer wide cylindrical region surrounding their trajectory, heavy ions create tracks resulting from Coulomb[3] and/or thermal spikes[4] accompanying the excitations, as shown by Monte Carlo[5] and molecular-dynamics simulations.[6] While laser beams are uniform at the nanoscopic level, ion beams can introduce substantial local anisotropic changes of structure and properties into solids. Tracks have been studied in homogeneous media that can be classified with respect to sensitivity to heavy-ion irradiation according to electronic properties. Macroscopic effects have been observed in thin films[7] where ion irradiation induces an anisotropic growth in the direction perpendicular to the beam without appreciable density change. This so-called "hammering" effect has been associated with shear strains resulting from transient thermal processes.[8] Oblate deformations in micrometer-size colloidal particles,[9] seen under MeV ion irradiation with low electronic stopping powers in the range 1–5 keV/nm, have also been attributed to this effect. At higher ion energies and electronic stopping powers, a nanometric-size effect on surface-deposited tin oxide powders irradiated with 4.6-MeV/nucleon Pb ions[10] has been reported. The largest grains (150 nm) were split into randomly oriented nanoclusters of 20 nm, while the smallest ones disappeared. No growth was observed.

Motivated by these contrasting observations, we have undertaken a study of the modifications undergone by nanometric aggregates embedded in solids when they are irradiated with heavy ions in the electronic stopping domain. Since the dynamic processes occurring during the spikes cannot be followed in real time, the clusters observed after irradiation may have been formed by self-reorganization after the initial violent spike destabilized the system. Such a mechanism combining cluster fragmentation and ripening has been described in a previous work[11] to explain the size modification of spherical Co nanoparticles embedded in a SiO_2 matrix by heavy-ion irradiation.

In this communication, we report on the change induced by ^{127}I ions of spherical nanometric Co particles embedded in SiO_2 layers to a prolate shape. The end result and proposed mechanism are completely different from the oblate deformations previously observed in microscopic colloids.[9] Besides the fundamental aspect of the deformation phenomenon, Co nanoparticles exhibit promising magnetic properties. Ion-beam techniques, as described in this work, represent a unique method for introducing oriented Co nanoparticles into microtechnology-compatible SiO_2 layers.

II. EXPERIMENTAL PROCEDURE

Dependence of nanoparticle size on implantation parameters has been studied previously,[11] and favorable conditions for the observation of transformations have been chosen. Co ions were first implanted at normal incidence into 300-nm-thick SiO_2 layers thermally grown on Si(100) wafers. The Co energy was 160 keV with a current density of $3\mu A\ cm^{-2}$ and a fluence of $10^{17}\ cm^{-2}$. The targets were mounted on a thermally isolated holder and heated with a defocalized halogen lamp to 873 K with the temperature controlled during implantation by a thermocouple. The Co nanoparticles have a mean diameter of 10 nm and adopt a fcc structure. The depth profile of the implanted species was measured by Rutherford backscattering spectroscopy (RBS).

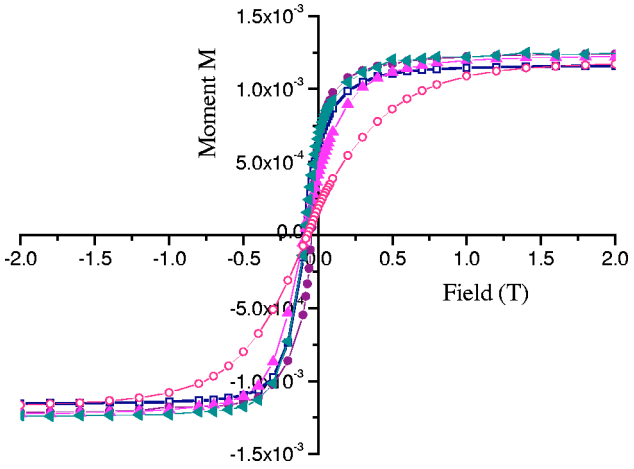

FIG. 1. Magnetic moment per unit area (10^{-3}A m^{-2}) as a function of the applied field measured at 5 K with a magnetic field applied perpendicular to the beam direction for the as-implanted sample (□), and the samples irradiated at 10^{11}(◀), 10^{12}(●), 10^{13}(▲), and 10^{14}(○) ^{127}I ions cm^{-2}.

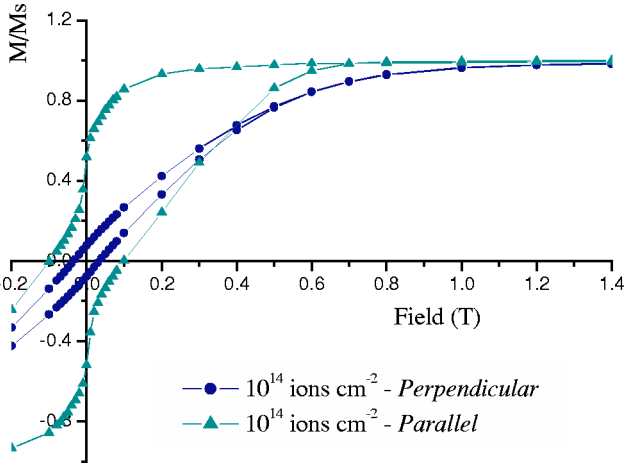

FIG. 2. Normalized magnetization measured at 295 K with a magnetic field applied perpendicular (●) and parallel (▲) to the beam direction for the sample irradiated at 10^{14} ^{127}I ions cm^{-2}.

The implanted samples were then irradiated at the Strasbourg Vivitron accelerator at room temperature with a scanned beam of 200-MeV ^{127}I ions at fluences ranging from 10^{11} to 10^{14} ions cm^{-2} at a flux of 3×10^{9} ions cm^{-2} s^{-1}. The magnetic properties of the samples were studied with a superconducting quantum interference device magnetometer at 295 and 5 K with a maximum field of 5 T applied perpendicular and parallel to the direction of the incident beams.

The size and shape evolution of the nanoparticles has been followed by transmission-electron microscopy (TEM) on thinned hand-polished cross-sectional specimens, at an acceleration voltage of 200 kV.

III. RESULTS

The range of 200-MeV ^{127}I in SiO_2 is 22 μm. Therefore the stopping power can be considered constant over the implanted layer. The total amount of Co in the layers, as determined by RBS, did not change with the ^{127}I irradiations.

The magnetic moment per unit area versus applied field measured at 5 K (Fig. 1) does not show a significant change in the saturation magnetization. Assuming that the saturation magnetization is that of bulk Co, this indicates that the total amount of metallic Co remains almost constant under irradiation. However, for high fluence ^{127}I irradiation, the shape of the curves changes. In Fig. 1, a small variation of slope can be noted at 10^{13} ions cm^{-2} and a clear difference is seen at 10^{14} ions cm^{-2}. The corresponding coercive fields H_c measured at 295 K increase (Table I).

In measurements on the samples irradiated at the highest fluences, H_c was higher (0.1 T) and the saturation magnetization was reached at a lower field with the magnetic field parallel to the irradiating beam than when the field was applied in the perpendicular direction (Fig. 2). This asymmetry suggests that high fluence irradiations induce modifications of the Co nanoparticle shape. The resulting macroscopic magnetic anisotropy shows that the easy axis is normal to the sample surface.

TEM observations showed a nanoparticle mean size increase in samples irradiated at ^{127}I fluences up to 10^{12} ions cm^{-2} but the particles remained spherical. However, modifications could be noticed for some nanoparticles irradiated at 10^{13} ions cm^{-2}, which then exhibit a lemon shape [Fig. 3(a)]. A more drastic change is seen after a higher fluence irradiation of 10^{14} ions cm^{-2}. In this case, particles are elongated along the direction of the propagation of the ions, i.e., normal to the surface [Fig. 3(b)]. Their mean dimensions are 9 nm in the direction parallel to the surface, and 35 nm in the perpendicular direction.

These observations are in agreement with the evolution deduced from the magnetic properties. At low fluence, the

TABLE I. Coercive fields H_c measured at 295 K for the as-implanted sample and the samples irradiated at 10^{13} and 10^{14} ions cm^{-2} with the magnetic field perpendicular ($\perp$) or parallel ($\|$)to the irradiation direction.

^{127}I fluence (ions cm^{-2})	0 (as implanted)	1×10^{13}	1×10^{14}	
$H_c(T)$	$\perp$ or $\|$	$\perp$ or $\|$	$\perp$	$\|$
	0.0105	0.0245	0.0345	0.1000

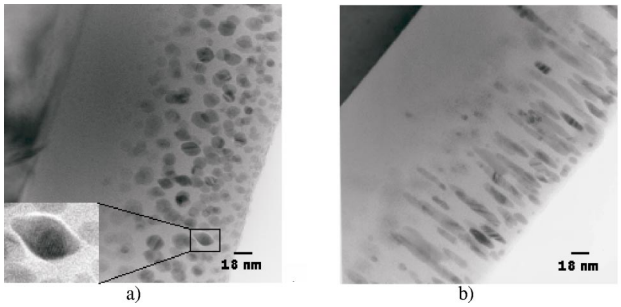

a) b)

FIG. 3. TEM micrographs of a sample irradiated at (a) 10^{13} and (b) 10^{14} ions cm^{-2}.

nanoparticles remain nearly spherical. The H_c, which is linked to magnetocrystalline anisotropy, depends only on cluster size and increases with it, as long as the clusters remain magnetic monodomains. At high fluence, when the clusters become elongated, a magnetic shape anisotropy appears, the easy axis being along the direction of elongation. Since this direction is the same for all nanoparticles, an observed macroscopic anisotropy results.

IV. DISCUSSION

The orientation of the deformed Co nanoparticles indicates that the mechanisms invoked in ion track formation could also be responsible for the anisotropic growth. Let us first consider the usual scenario for track formation: Coulomb explosion occurs at 10^{-15}–10^{-13} s after passage of the ^{127}I ion, followed by the thermal spike at 10^{-13}–10^{-11} s, and plastic flow[12]at 10^{-10}–10^{-9} s. Due to the observed elongation parallel to the beam direction, in opposition to conventional plastic deformation,[9] we assume that such plastic deformations inside the nanoparticles do not cause the anisotropy in our case. Since most of the energy initially deposited near the track by Coulomb interactions is progressively thermalized, we compare the heat evolution in the metallic nanoparticle with that in the surrounding insulating medium. The transit time of a 200-MeV ^{127}I ion through a 10-nm Co cluster is of the order of 10^{-15} s. In the framework of the thermal spike model, the temperatures of the hot electrons and of the lattice are given by a system of two coupled equations.[4] After the initial energy injection (10^{-15} s), heat propagates in the electronic subsystem with a diffusion coefficient[13] $D_e \sim 2$ cm^2 s^{-1} corresponding to a diffusion time of 10^{-13}–10^{-14} s in a 10-nm-diameter nanoparticle, whereas the characteristic electron-phonon transfer time is 10^{-12}–10^{-13} s. Afterwards, the heat transferred to the lattice via electron-phonon coupling propagates in the lattice. Taking into account the time evolution of the different processes, and assuming that the hot electrons are confined in the metallic Co nanoparticles, the following simplifications can be made:

(i) in $\sim 10^{-13}$ s, the electrons in the Co nanoparticles reach a constant temperature corresponding to an equilibrium of the energy transferred by the ion to the electrons,

(ii) in $\sim 10^{-12}$ s, this energy is transferred to the Co lattice, and the nanoparticle reaches an initial temperature T_0, and

(iii) after 10^{-12} s, the heat propagates to the surrounding insulating medium.

The variation of T_0 with nanoparticle diameter is shown in Fig. 4. The following simplifications were made: (i) all the energy loss of the incident ion in the nanoparticle is transferred to the atoms during the thermalization process, (ii) size effects on the thermal properties are neglected, and (iii) thermal constants of bulk material in normal conditions are used. In practice, even drastic modifications of these parameters do not modify the general behavior described below. As seen in Fig. 4, the initial temperature T_0 of a Co nanoparticle

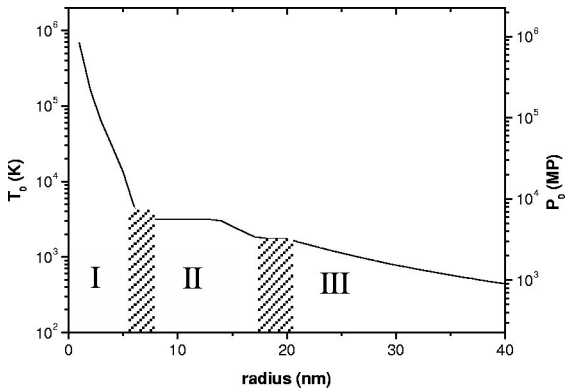

FIG. 4. Radial dependence of the initial temperature T_0 and pressure P_0 of a spherical Co nanoparticle traversed by a 200–MeV ^{127}I ion. Plateaus indicate the fusion and vaporization transitions for bulk material under normal conditions. The curve was calculated assuming that all the energy lost by the ion is converted into thermal effects. Regions I, II, and III are explained in Sec. IV and are separated by cross hatching to show the uncertainty due to the approximations.

decreases with increasing radius. In region I, for radii below 6–8 nm, the temperature corresponds to vaporization (of free particles), and under such high mean energies per atom it is assumed that nanoparticles explode into fragments and/or atoms. These fragments or atoms aggregate themselves around spherical clusters in their vicinity by Ostwald ripening. For this reason, in region I nanoparticles grow in size and the total amount of metallic Co remains unchanged. In region II, from 6–8 to 18–20 nm, particles are molten during the time interval 10^{-12}–10^{-11} s. Thermal spike calculations for amorphous SiO_2, represented in Fig. 5, show that the temperature in the center of the track in the insulating material is higher than that in the nanoparticles. However, due to differences in volume expansion and compressibility, there is a large overpressure in the molten Co particle (P_0 in Figs. 4 and 5 is calculated according to Ref. 10) and a creep deformation of the particle is induced. After the deformation, the shape is frozen-in during the cooling of the material in 10^{-11}–10^{-8} s. In region III of Fig. 4, which has not been investigated here, larger particles remain in the solid phase.

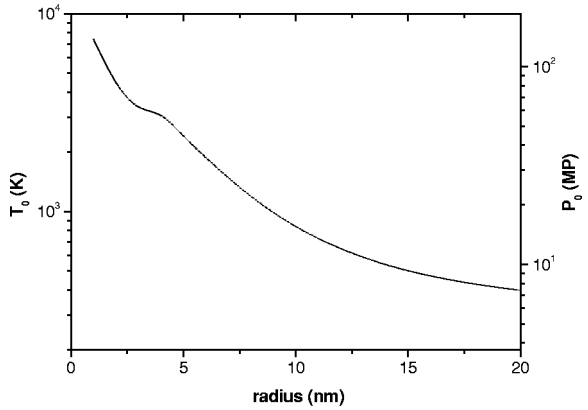

FIG. 5. Temperature T_0 and pressure P_0 as a function of distance from the track axis in SiO_2 at 10^{-12} s after the energy deposition to the electrons.

Our experimental results can be understood using the general approach described above. Starting with small radius nanoparticles in region I, irradiations with energetic ions induce growth by fragmentation and ripening until the nanoparticles reach a critical diameter corresponding to the transition from region I to II at fluences near 10^{13} cm^{-2} for ^{127}I. Above this fluence, each projectile impact contributes to an increase of the asymmetry. Finally, coalescence of elongated particles at fluences of 10^{14} cm^{-2} can lead to the formation of nanoparticles that are more massive than the initial individual spherical clusters. Accompanying these violent spike effects, irradiation-induced stress[14] or/and irradiation-enhanced and thermally activated diffusion of ejected particles along the ion track may also contribute to a preferential growth in the track direction. The relative importance of each contribution remains to be determined.

From a fundamental point of view, fragmentation and melting processes occurring in embedded nanoparticles, as described here, have been related to the behavior of free clusters or nuclei breaking up into fragments during their transition to a gas, and local high-energy-induced multifragmentation can be regarded as a general characteristic of phase transitions in nanoparticles as well as in high-energy nuclear physics phenomena.

V. CONCLUSION

We have shown that high-energy ion irradiation can modify the morphology of metallic Co nanoparticles formed by a previous ion implantation. After heavy-ion irradiation at low fluence (10^{11} and 10^{12} ions cm^{-2}), the nanoparticles grow in size but remain spherical. At higher fluences (10^{13} and 10^{14} ions cm^{-2}), growth along the incident-beam direction is observed. The size modification and the prolate deformation have been explained in the framework of the thermal spike model.

ACKNOWLEDGMENTS

The authors would like to thank Y. Le Gall for the Co implantations and the Vivitron team for providing scanned ^{127}I beams for the irradiations.

[1] R.L. Johnson, *Atomic and Molecular Clusters* (Taylor & Francis, London, 2002).

[2] C. Bréchignac, Ph. Cahuzac, F. Carlier, M. de Frutos, N. Kébayli, J. Leygnier, A. Sarfati, and V. Akulin, in *Large Clusters of Atoms and Molecules*, edited by T. P. Martin (Kluwer Academic, Dordrecht, 1996), Vol. 313, p. 315, and references therein.

[3] R.L. Fleischer, P.B. Price, and R.M. Walker, *Nuclear Tracks in Solids* (University of California, Berkeley, 1975).

[4] I.M. Lifshitz, M.I. Kaganov, and L.V. Taratanov, J. Nucl. Energ. Parts A/B **12**, 69 (1960).

[5] B. Gervais and S. Bouffard, Nucl. Instrum. Methods Phys. Res. B **88**, 355 (1994).

[6] E.M. Bringa and R.E. Johnson, Phys. Rev. Lett. **88**, 165501 (2002).

[7] S. Klaumunzer and G. Schumacher, Phys. Rev. Lett. **51**, 1987 (1983).

[8] H. Trinkaus and A.I. Ryazanov, Phys. Rev. Lett. **74**, 5072 (1995).

[9] T. van Dillen, E. Snoeks, W. Fukarek, C.M. van Kats, K.P. Velikov, A. Blaaderen, and A. Polman, Nucl. Instrum. Methods Phys. Res. B **175**, 350 (2001).

[10] A. Berthelot, S. Hemon, F. Gourbilleau, C. Dufour, E. Dooryhee, and E. Paumier, Nucl. Instrum. Methods Phys. Res. B **146**, 437 (1998).

[11] C. D'Orléans, C. Cerruti, C. Estournès, J.J Grob, J.L. Guille, F. Haas, D. Muller, M. Richard-Plouet, and J.P. Stoquert, Nucl. Instrum. Methods, Phys. Res. B (published online 16 March 2003).

[12] A.I Ryazanov, A.E. Volkov, and S. Klaumunzer, Phys. Rev. B **51**, 12 107 (1995).

[13] C. Dufour, A. Audouard, F. Beuneu, J. Dural, J.P. Girard, A. Hairie, M. Levalois, E. Paumier, and M. Toulemonde, J. Phys.: Condens. Matter **5**, 4573 (1993).

[14] A. Guntzmann and S. Klaumunzer, Nucl. Instrum. Methods Phys. Res. B **127/128**, 12 (1997).